THE JOURNAL OF PHYSICAL CHEMISTRY Letters

Letter

pubs.acs.org/JPCL

($\pi\pi^*/\pi\sigma^*$) Conical Intersection Seam Experimentally Observed in the S−D Bond Dissociation Reaction of Thiophenol-d_1

Hyun Sik You,[†] Songhee Han,[†,‡] Jean Sun Lim, and Sang Kyu Kim*

Department of Chemistry, KAIST, Daejeon 305-701, Republic of Korea

Supporting Information

ABSTRACT: Surface crossing of bound (S_1, $\pi\pi^*$) and continuum (S_2, $\pi\sigma^*$) states has been observed in the ultrafast S−D bond dissociation reaction of thiophenol-d_1. It is manifested by an unanticipated variation of fragment angular distribution as a function of the excitation energy. The anisotropy parameter (β) of +0.25 at the S_1 origin decreases to −0.60 at ∼600 cm^{-1} above the S_1 zero-point level, giving a broad peak in β with a bandwidth of ∼200 cm^{-1}. The peak in β is ascribed to the in-plane S-D bending mode excitation by which the nuclear configuration in the proximity of the S_1/S_2 conical intersection seam is directly accessed, showing a mixed character of parallel (S_1-S_0) and perpendicular (S_2-S_0) transition dipole moments at the same time. As a result, the dynamic aspect of the conical intersection is experimentally revealed here through direct access to the nuclear configuration on the multidimensional conical intersection seam.

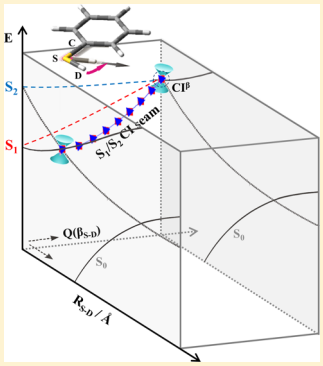

Chemical reactions are often described as nuclear movements of which directions and speeds are determined by shapes of multidimensional electronic potential energy surfaces. This adiabatic picture is based on the seminal Born−Oppenheimer approximation that assumes that the nuclear motion is separable in time from the much faster electronic motion.[1] The Born−Oppenheimer approximation has been enormously successful in describing chemical reactions on the ground electronic state. For chemical reactions on the electronically excited states, however, coupling of electronic and nuclear motions becomes nontrivial, and significant nonadiabatic transitions where nuclear motions induce surface-hopping (and vice versa) occur in many circumstances.[2] Nonadiabatic transitions are ubiquitous in nature and even essential in a number of important chemical and biological processes.[3−6] Notably, for polyatomic molecules, the noncrossing rule does not strictly apply and a conical intersection point is generated by intersection of two potential curves on the 2D branching plane. In general, the conical intersection lies on the ($3N-8$) dimensional seam, where ($3N-6$) is the number of internal degrees of freedom of N atomic molecular system.[7−9] As the energy gap between two adiabatic potential surfaces becomes infinitesimally small in the proximity of conical intersections, nonadiabatic transitions are facilitated when the reactive flux or wavepacket reaches the conical intersection region during the chemical reaction process. Most dynamic outputs of nonadiabatic transitions are then dictated by the nature of the conical intersections, and it would be extremely valuable if one could figure out the structure and dynamic role of conical intersections.

In this regard, there have been numerous theoretical and experimental studies on conical intersection dynamics in recent decades. Theoretical descriptions of conical intersections have been very successful in explaining many important nonadiabatic chemical processes. These include photochemical organic reactions,[10] photoisomerization,[11,12] the radiation-protecting mechanism of DNA bases,[13,14] or photodissociation reactions.[15,16] Spectroscopic perturbations observed in photoabsorption or photoionization have given strong experimental evidence of the existence of conical intersections.[9,17] Nonadiabatic channels have been thoroughly investigated in terms of nonadiabatic transition probability and associated dynamic properties such as energy disposal and reaction rates for many chemical reactions.[16,18−23] Recent time-domain studies have revealed wavepacket motion undergoing surface hopping between two diabats for small or complex systems, giving the real-time movies of the nonadiabatic transition processes.[24]

Despite many important and successful experimental results to date, however, it is still extremely difficult to unravel the structure and dynamics of a multidimensional conical intersection experimentally. For photodissociation reactions, to our best knowledge, the structural property of the conical intersection had not been spectroscopically characterized before our recent report on the $\pi\sigma^*$ mediated dissociation of thioanisole ($C_6H_5SCH_3$).[21,25] In the photodissociation of thioanisole, the nonadiabatic transition probability shows resonances at the vibronic transitions that allow the initial reactant flux to access the conical intersection region. The structural aspect of the conical intersection is then inferred from the nature of the vibronic states associated with resonances in the nonadiabatic transition probability.

Received: July 5, 2015
Accepted: August 3, 2015

DOI: 10.1021/acs.jpclett.5b01420
J. Phys. Chem. Lett. 2015, 6, 3202−3208

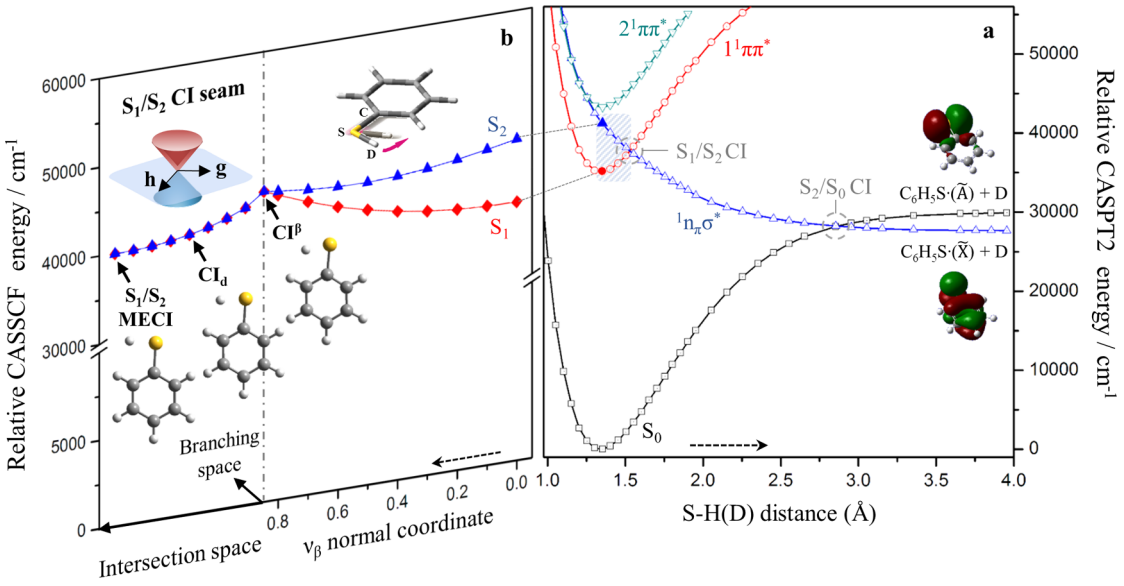

Figure 1. (a) Four lowest potential energy curves (S_0, $1^1\pi\pi^*$, $^1n_\pi\sigma^*$, and $2^1\pi\pi^*$) of thiophenol(-d_1) along the S−H(D) bond elongation at the planar geometry, obtained by the CASPT2//SA4-CASSCF(12,11)/6-311++G(d,p) level. (b) SA4-CASSCF(12,11) potential energy profiles of the first (S_1) and second (S_2) electronically excited states along the in-plane SD bending (ν_β) normal coordinates (relevant nuclear displacements are shown) and the linearly interpolated path (intersection space) connecting CI^β and the S_1/S_2 MECI. The vertical dashed line separates the two different coordinates. The S_1/S_2 conical intersection seam is generated along the intersection space that is orthogonal to the 2D branching space (see Figure S5). The geometries (CI^β, CI_d, and S_1/S_2 MECI) on the conical intersection seam are shown along the path.

Herein, we report another example of the spectroscopic characterization of the conical intersection on the multidimensional seam, in this case by the observation of the resonance-like features in the product angular distribution from the photodissociation reaction of thiophenol-d_1 (C_6H_5SD). Thiophenol adopts a planar geometry at both ground and first electronically excited states.[16,26] The S−H(D) bond dissociation of thiophenol in S_1 occurs through coupling to the repulsive S_2 ($\pi\sigma^*$) state.[27−30] In the planar geometry, as shown in Figure 1a, two conical intersections are encountered along the S−D bond dissociation pathway. The S_1/S_2 conical intersection opens the gate to the chemical reaction for the reactant that is initially bound in the S_1 state. At the second S_0/S_2 conical intersection, the reactive flux (or wavepacket) gives rise to the $C_6H_5S·(\tilde{A})$ fragment adiabatically, whereas the $C_6H_5S·(\tilde{X})$ fragment is produced by a nonadiabatic transition. The S_0/S_2 conical intersection is located with a short S−D bond distance of ∼1 Å from the S_1/S_2 conical intersection. Therefore, the quantum natures of two conical intersections are closely related to each other. Our report here on detailed dynamics of thiophenol-d_1 on the close-lying S_1 and S_2 states reveals a new dynamic facet for chemical reactions taking place near the conical intersection.

Observation of a Resonance-Like Feature in the Product Angular Distribution. The S−H(D) bond cleavage of thiophenol is prompt, as evidenced by the absence of a resonance-enhanced multiphoton ionization signal with the nanosecond laser pulse. Instead, the photofragment excitation (PHOFEX) spectrum, which monitors the $C_6H_5S·$ fragment yield as a function of the excitation energy, gives the S_1 origin band of which the full-width at half-maximum (fwhm) is ∼190 cm^{-1}, which corresponds to an S_1 lifetime of ∼50 fs (see Figure S2). This result is consistent with the previously reported action spectra that were taken by probing the H(D) fragment from thiophenol(-d_1).[29] Ultrafast S−D bond rupture should be then reflected in the angular distribution of fragments as the linearly polarized pump laser pulse interacts with the transition dipole moment of which the direction is well-defined with respect to the dissociating S−D bond axis. According to our time-dependent density function theory (TDDFT) or complete active space second-order perturbation theory (CASPT2) calculation,[30] the S_1-S_0 transition dipole moment is parallel to the benzene plane, whereas it is tilted about 20° or 53° from the S−D bond axis (see Supporting Information), respectively. As the bond breakage occurs much faster than the rotational period, the anisotropy parameter (β) from $I(\theta) = (\sigma/4\pi)[1 + \beta P_2(\cos\theta)]$ is expected to be positive for the angular distribution of D from the S_1 thiophenol-d_1. Here θ is the angle between the direction of the fragment velocity and the electric vector of linearly polarized light, σ is the absorption cross section, and $P_2(\cos\theta)$ is the second Legendre polynomial. Actually, the anisotropy parameter is estimated to be +0.25 at the S_1 zero-point level, and this is more consistent with the CASPT2 calculation, as shown in Figure 2c. Surprisingly, however, it is found that β deceases sharply with increasing of the S_1 internal energy to give the negative value of −0.60 before going back to nearly zero again, giving a broad peak ($\Delta E \approx 200$ cm^{-1}) in β centered at the S_1 internal energy of ∼600 cm^{-1}. Interpretation of this rather peculiar behavior of β varying with the internal energy in the same electronic state is not straightforward, as a number of dynamic parameters are associated in the angular distribution of fragments. An abrupt change of the reaction rate, accompanied by a change of β, should be excluded as the S−D bond breakage occurs much faster than the rotational period over the entire S_1 excitation energy range. As the excitation energy increases, vibrational modes activated in the vertical transition could be projected in both the angular and speed distributions of the products because the S−D bond rupture is much faster than the energy randomization process; however, it is not likely that any particular vibrational mode excitation could give such a negative

DOI: 10.1021/acs.jpclett.5b01420
J. Phys. Chem. Lett. 2015, 6, 3202−3208

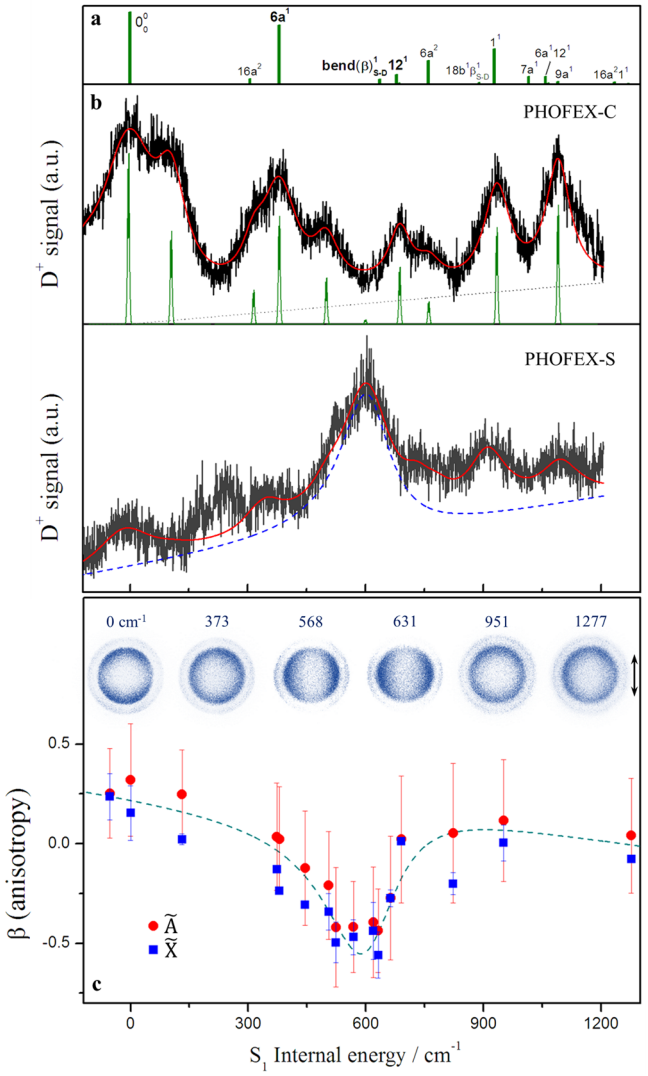

Figure 2. (a) Franck–Condon simulation spectrum of the S_1–S_0 transition obtained using the TDDFT (B3LYP)/aug-cc-pVTZ. Vibrational mode assignments are also given. Vibronic transitions at ~105, ~310, and ~500 cm^{-1} above the S_1 origin in the PHOFEX spectrum are not properly assigned at the present time. A Franck–Condon-simulated spectrum based on the SA4-CASSCF/6-311++G(3df,3pd) calculation is somewhat different and shown in the Supporting Information for the comparison (Figure S1). (b) PHOFEX-C (upper trace) and PHOFEX-S (lower trace) spectra taken by probing the D fragment at wavelengths corresponding to center and red edge of the Doppler profile, respectively (see the text for details). Rotational contours convoluted with the laser bandwidth are shown as green lines. Lorentzian functions are used for the simulation of PHOFEX spectra as shown in red curves (see the Supporting Information). (c) Anisotropy parameter (β) values averaged over the fwhm of the translational energy peak associated with the $\tilde{X}$ (blue squares) or $\tilde{A}$ (red circles) states of the thiophenoxyl radical. An asymmetric line was used for the fit (cyan dotted line). Raw images taken at S_1 internal energies (E_{ph} − 34 990 cm^{-1}) of 0 (origin), 373, 568, 631, 951, and 1277 cm^{-1} are shown. The black arrow indicates the polarization direction of the pump laser pulse.

β value, especially because only in-plane modes are symmetrically allowed in the S_1–S_0 transition of thiophenol.

Probing the Structure and Dynamics of the Conical Intersection. The β-dip is then only explainable by invoking the S_2–S_0 transition dipole moment of which the direction is perpendicular to both the benzene plane and the S–D bond axis. Namely, the β-dip is ascribed to the coherent superposition of the S_1–S_0 and S_2–S_0 transitions. It should be emphasized here that the energetic coincidence of excitation energy and the S_1/S_2 conical intersection seam is a necessary but not sufficient condition for the S_1/S_2 coherent excitation. More importantly, the nuclear configuration near or at the conical intersection seam should be accessed by the optical excitation to observe the mixed character of parallel (S_1–S_0) and perpendicular (S_2–S_0) transition dipole moments. Actually, the S_2–S_0 vertical excitation starts to be active only when the excitation energy is ~2000 cm^{-1} above the S_1 origin (vide infra). Therefore, the β-dip at 600 cm^{-1} above the S_1 origin should be due to the excitation of a particular vibronic band through which the nuclear configuration near the S_1/S_2 conical intersection seam is accessed.

We have obtained two different PHOFEX spectra of thiophenol-d_1. In taking velocity-map ion images, the probe laser wavelength for (2 + 1) ionization of the D fragment was continuously scanned to cover the entire Doppler broadened spectral width. Because the polarization axis of the pump laser pulse is set to be perpendicular to the propagation axis of the probe laser pulse, the center wavelength of the Doppler profile is more sensitive to the D fragment produced from the parallel transition with $\beta > 0$ (center column of the image), whereas D from the perpendicular transition with $\beta < 0$ is more sensitive to the wavelength at blue- or red-edge of the Doppler profile (side column of the image). The PHOFEX spectrum taken by monitoring the center column of the image (PHOFEX-C) then most likely represents absorption cross section of parallel transition, while the PHOFEX spectrum obtained by monitoring the side column of the image (PHOFEX-S) is more likely to be associated with the absorption cross section of perpendicular transition. Indeed, spectral patterns of PHOFEX-C and PHOFEX-S are quite different (Figure 2). As expected, because S_1–S_0 is parallel transition with $\beta > 0$, all of Franck–Condon active S_1 vibronic transitions are observed in the PHOFEX-C spectrum. This matches perfectly well with the PHOFEX spectrum previously reported by the Ashfold group,[29] and our Franck–Condon calculation gives the proper mode assignments for most of the observed bands. Apparently, however, the β peak does not match any strongly observed peak in the PHOFEX-C spectrum. Because all observed bands are very broad, however, it should be noted that weak S_1 vibronic bands are hardly identified. The absorption cross section of the vibronic transition associated with the β dip therefore is expected to be quite small in terms of the Franck–Condon overlap.

The situation becomes different in the PHOFEX-S spectrum, where intensities of parallel vibronic transitions decrease whereas those of perpendicular transitions stand out. Interestingly, a distinct vibronic band at ~600 cm^{-1} above the origin has been clearly identified in the PHOFEX-S spectrum (Figure 2). Actually, this vibronic band in PHOFEX-S matches exactly with the anisotropy parameter (β) dip in terms of both peak position and width. This experimental finding strongly indicates that the β dip at 600 cm^{-1} is not due to intensity-borrowed statistically mixed S_2–S_0 transition. Namely, if that was the case, no discernible vibronic structure would be observed in the PHOFEX-S spectrum as the S_2–S_0 transition is bound-to-continuum in nature.

The most plausible vibronic band responsible for the β dip could then be the ν_β mode, which is associated with the in-

DOI: 10.1021/acs.jpclett.5b01420
J. Phys. Chem. Lett. 2015, 6, 3202–3208

Table 1. Critical Geometrical Parameters and Relative Energies of Thiophenol-d_1 at the Ground (S_0), First Excited State (S_1), Classical Turning Points of the ν_β = 1 state (S_1^β), CIs along the ν_β Normal Coordinate (CI^β), and S_1/S_2 MECI[d]

	Equilibrium				
	$S_{0\ min}$	$S_{1\ min}$	$S_1^{\beta\ a,b}$	CI^β	S_1/S_2 MECI
	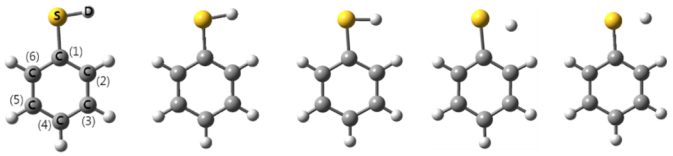				
Relative energy (ΔE, cm^{-1})	0	37121 38403[c]	38178 (38170)	44246	39958
d(S-D) (Å)	1.354	1.355	1.38 (1.37)	1.46	1.55
$\gamma(C_1\text{-S-D})$ (deg)	96.6	97.0	85.5 (103.9)	72.5	91.1
$d(C_1\text{-S})$ (Å)	1.80	1.78	1.83 (1.76)	1.81	1.78
$\gamma(C_2\text{-}C_1\text{-S})$ (deg)	122.9	122.2	121.6 (122.5)	125.1	123.0
$d(C\text{-}C)_{av}$ (Å)	1.40	1.44	1.44 (1.43)	1.40	1.42

[a]Geometrical parameters of the classical turning point are obtained at the vibrational energy of ~$3/2E_\nu$ above the S_1 minimum energy along the ν_β normal coordinate, where E_ν corresponds to one quantum of the ν_β mode. [b]Values in parentheses represent the other end geometry of the classical turning point. [c]S_1-S_0 vertical excitation energy at the S_0 minimum energy geometry. [d]Ab initio values are obtained at the SA4-CASSCF(12,11)/6-311++G(d,p) level.

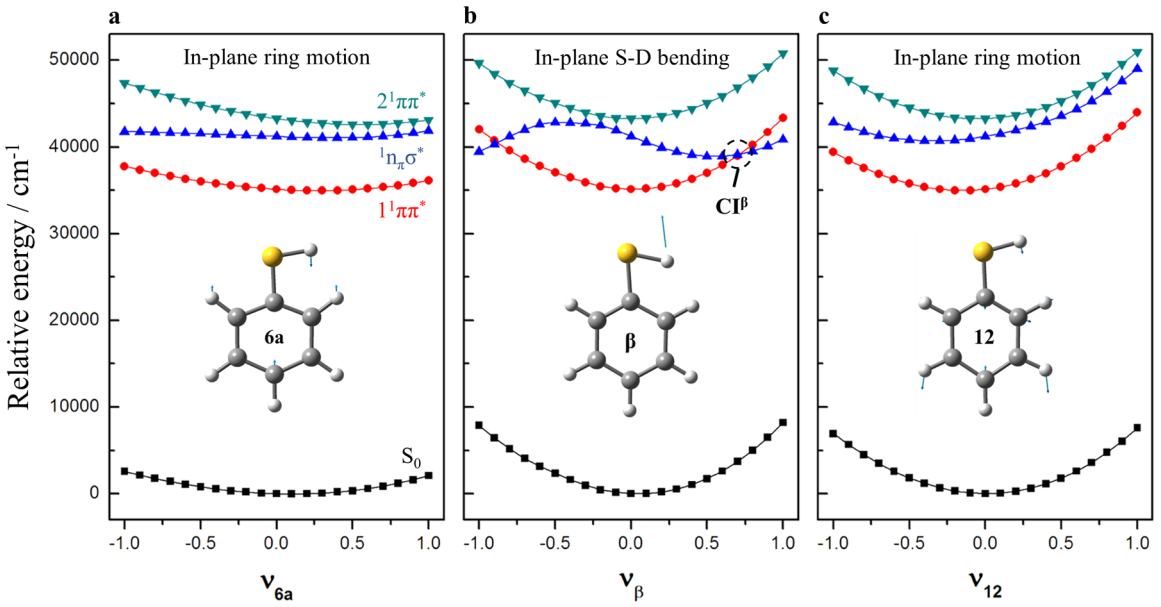

Figure 3. Potential energy curves of the S_0, $1^1\pi\pi^*$, $^1n_\pi\sigma^*$, and $2^1\pi\pi^*$ in thiophenol-d_1 as a function of the (a) ν_{6a}, (b) ν_β, and (c) ν_{12} normal coordinates, calculated at the CASPT2//SA4-CASSCF(12,11)/6-311++G(d,p) level. The conical intersection (CI^β) of S_1 ($\pi\pi^*$) and S_2 ($n_\pi\sigma^*$) electronic states is found only for the in-plane SD bending (ν_β) normal coordinate. The CI^β is calculated to be 4045 cm^{-1} above the S_1 minimum energy. Nuclear displacement vector descriptions of corresponding normal modes are shown.

plane S-D bending motion. Energetically, ab initio calculation gives a value of 680 cm^{-1} for ν_β. Considering anharmonicity, which is expected to be large near the conical intersection, the ν_β assignment for the β dip at 600 cm^{-1} is quite reasonable energetically. Now, how about the nuclear configuration spanned by the ν_β mode excitation? According to our calculations, the S_1/S_2 minimum energy conical intersection (MECI) adopts a molecular geometry in which the dissociating S−D bond is elongated whereas the C−S−D in-plane angle is reduced from the equilibrium value, as shown in Table 1. Interestingly, the classical turning point reached by one quantum of the ν_β mode excitation represents a molecular geometry with an elongated S−D bond length and reduced C−S−D in-plane angle with respect to the S_1 minimum energy structure. This indicates that the ν_β mode excitation prepares the reactive flux on the nuclear configuration near the conical intersection seam, which is connected to the MECI point (Figure 1b).

DOI: 10.1021/acs.jpclett.5b01420
J. Phys. Chem. Lett. 2015, 6, 3202−3208

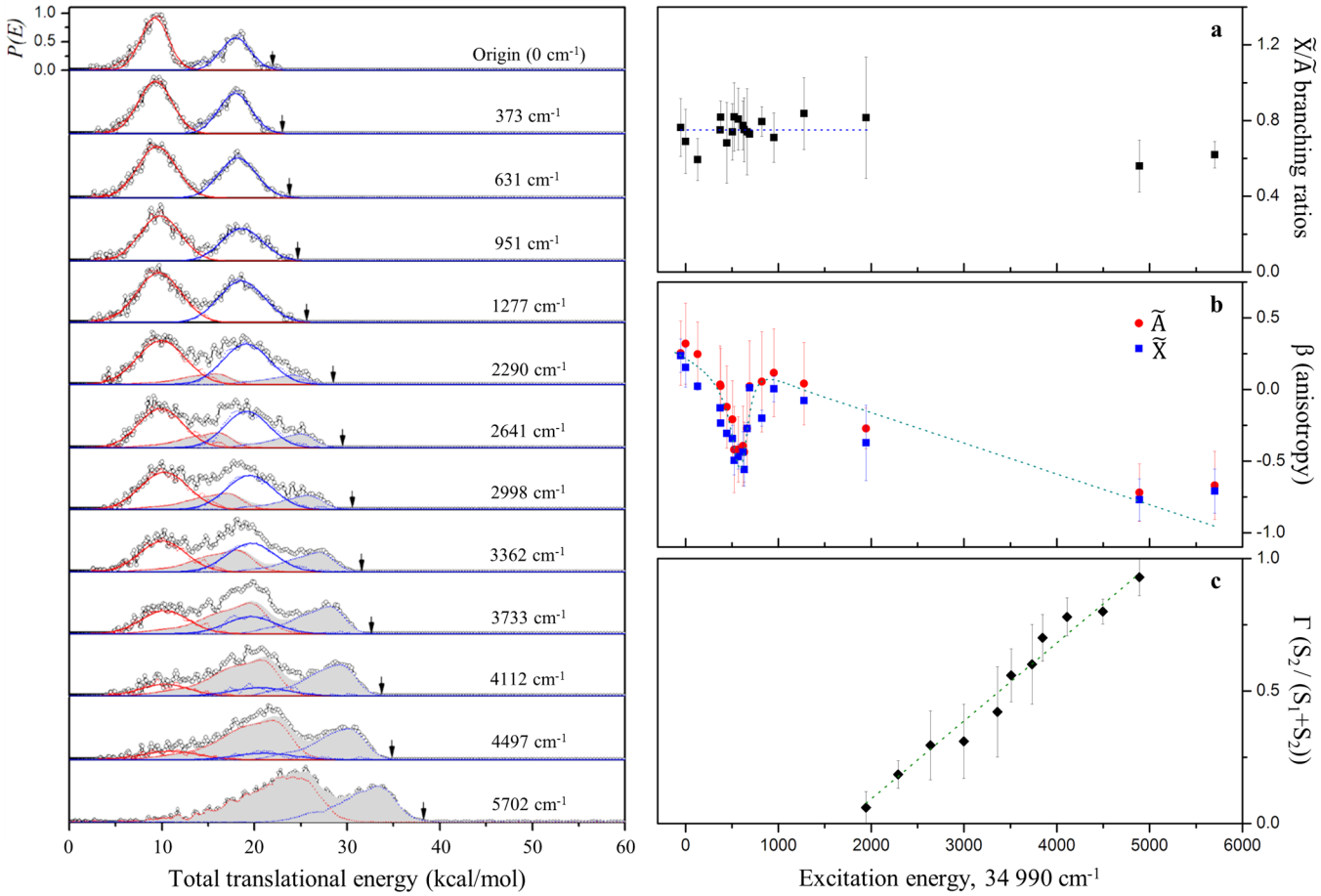

Figure 4. Left: Total translation energy distributions of the nascent D fragment after the subtraction of the background signal due to the probe laser only at various excitation energies. Photolysis energies minus the S_1 origin of 34 990 cm^{-1} are depicted for each translational energy distribution. The product state distributions associated with the $\tilde{X}$ (blue) and $\tilde{A}$ (red) states of $C_6H_5S\cdot$ are deconvoluted from the experiment (open circles). Contributions from the S_1-S_0 excitation (solid lines) and the S_2-S_0 vertical excitation (shaded) are also deconvoluted from the experimental result. (See the text for further details.) Black arrows indicate maximum available energies when the S−D bond dissociation energy is taken to be 27 308 cm^{-1}. Right: (a) $\tilde{X}/\tilde{A}$ branching ratios, (b) β values averaged over the fwhm of the translational energy distribution associated with the $\tilde{X}$ (blue squares) or $\tilde{A}$ (red circles) state of the thiophenoxyl radical, and (c) the fraction (Γ) of the S_2-S_0 vertical transition (black diamond with a green dotted line) in the total absorption cross-section as a function of excitation energy up to ~6000 cm^{-1} above the S_1 origin.

It should be noted that the simple potential energy curve with two curve crossing points, depicted in Figure 1a, is just a 1D projection of the complicated multidimensional potential energy surfaces on the S−D bond elongation coordinate. Actually, because there are 33 normal modes for thiophenol, the projection of the multidimensional potential energy surfaces on each normal mode coordinate will produce 33 different potential energy curves. Obviously, not all of these curves produce surface crossing points. Here we calculate the potential energy curves along the nuclear displacements associated with ν_{6a}, ν_β, and ν_{12} normal modes. The ν_{6a} and ν_{12} are in-plane ring modes of which the vibrational frequencies are slightly lower (380 cm^{-1}) or higher (690 cm^{-1}), respectively, than that of ν_β at 600 cm^{-1}. Interestingly, it is found that the S_1/S_2 curve crossing occurs only for the potential energy curve projected on the ν_β mode coordinate. Potential energy curves along the ν_{6a} or ν_{12} normal mode coordinates do not generate curve crossings between S_1 and S_2, as shown in Figure 3. The S_1/S_2 conical intersection point along the ν_β normal-mode coordinate (CI^β) theoretically lies on the same conical intersection seam as the MECI point. Namely, both CI^β and MECI are on the same branching plane, where the gradient difference vector is parallel to the S−D stretching and the derivative coupling vector is associated with CCSD dihedral torsion. Actually, CI^β and MECI are smoothly connected on the same branching plane without a barrier to generate a conical intersection seam, as can be seen in Figure 1b. Therefore, our calculations support the idea that ν_β mode excitation is responsible for the experimentally observed β-dip, which results from direct access to the conical intersection seam. As previously mentioned, the peak position and bandwidth of the β-dip are almost identical to those of the PHOFEX-S vibronic band within the error limit, which is also consistent with the above argument. Actually, this vibronic band at 600 cm^{-1} seems to be slightly asymmetric in shape, and this could possibly be due to interference of two coherent transitions, although further studies are definitely needed.[31−33] The simple potential energy curve, drawn as a function of the S−D bond elongation coordinate, gives the S_1/S_2 crossing point at ~1802 cm^{-1} above the minimum energy level of S_1 according to the CASPT2 calculation.[34] Considering the zero-point energy (ZPE) difference between S_1 and S_2 with respect to the S−D stretching mode, the S_1/S_2 curve crossing is calculated to be ~850 cm^{-1} above the S_1 ZPE level. This somewhat low barrier to the S_1/S_2 curve crossing explains the prompt S−D bond rupture dynamics quite well, yet, the

DOI: 10.1021/acs.jpclett.5b01420
J. Phys. Chem. Lett. 2015, 6, 3202−3208

energetics involved in the conical intersection calculations need to be improved from the values presented here.

Now, we need to consider symmetries of excited states involved in nonadiabatic transitions. The S−D bond dissociation of the S_1 thiophenol-d_1 takes place via tunneling through a reaction barrier, which is generated by the S_1/S_2 ($\pi\pi^*/\pi\sigma^*$) conical intersection. This means that the optically prepared S_1 (A') should be coupled to S_2 (A'') in the C_s point group. Therefore, out-of-plane vibrational modes (a'') in S_2 are expected to be activated as the reactive flux passes through conical intersections along the S−D bond dissociation pathway. For most distinctly observed S_1 vibronic bands in the PHOFEX-C spectrum, this nonadiabatic vibronic coupling is believed to occur, as had already been discussed in previous studies;[28−30] however, for the 600 cm^{-1} band, which is distinctly observed in the PHOFEX-S spectrum, the situation is somewhat different. Namely, as previously described, the $\pi\pi^*/\pi\sigma^*$ conical intersection seam is extended into the Franck−Condon region accessed by the ν_β mode excitation (Figure 1), and thus both S_1 (A') and S_2 (A'') are optically excited simultaneously with the parallel ($\beta > 0$) or perpendicular ($\beta < 0$) transition dipole moment, respectively, rationalizing the experimentally observed β-dip very nicely.

At the S_1 origin, the product branching ratio of $C_6H_5S\cdot(\tilde{X})$ to $C_6H_5S\cdot(\tilde{A})$ is estimated to be ∼0.75 ± 0.15 and remains constant in the S_1 internal energy range of 0−2000 cm^{-1}, indicating that the nonadiabatic transition probability at the S_0/S_2 conical intersection is quite high and the ultrafast S−D bond rupture takes place without any significant energy flow into the critical vibrational modes relevant to the change of the S_1/S_2 coupling strength. This suggests that the S−D bond cleavage of thiophenol-d_1 may take place without strong torque along the C_2-C_1-S-D dihedral torsional angle, implying that out-of-plane ring modes may then be actively involved in symmetry-constrained vibronic coupling process. Interestingly, starting at ∼2000 cm^{-1} above the S_1 origin, the product translational energy distribution shows a sharp shoulder in the high-energy region, indicating that a new dynamic channel starts to open at around this energy, as shown in Figure 4. This feature becomes more pronounced at ∼3000 cm^{-1} above the origin, giving a third peak representing the $C_6H_5S\cdot(\tilde{X})$ fragment produced from the new channel, whereas the translational distribution of $C_6H_5S\cdot(\tilde{A})$ from the new channel overlaps with that giving $C_6H_5S\cdot(\tilde{X})$ from the S_1 channel at the center peak. As the energy increases, the Gaussian-shaped product state distribution from the S_1 channel diminishes, whereas the product state distribution, which has a higher translational partitioning ratio, becomes dominant. This experimental fact indicates that the new channel is due to the vertical excitation to the high-lying repulsive S_2 state as the direct dissociation naturally gives more translational energy to the fragments. This is also consistent with the theoretical S_2-S_0 vertical excitation energy of 4803 cm^{-1} above the S_1 origin (Table S7). The negative anisotropy parameter of -0.73 ± 0.05, measured at ∼4900 and ∼5700 cm^{-1} above the S_1 origin, is also consistent with the direction of the S_2-S_0 transition dipole moment, which is perpendicular to the molecular plane on which the S−D bond axis is placed. The distinctly different dynamics of the two channels allow the deconvolution of the total translational energy distribution of the nascent fragments into individual contributions from the S_1-S_0 and S_2-S_0 transitions. Intriguingly, the increase in the S_2-S_0 vertical-transition component with increasing excitation energy is quite well correlated with the decrease in the anisotropy parameter of the product angular distribution, as can be seen in Figure 4. The β dip at 600 cm^{-1} therefore is due to simultaneous excitation of S_1 and S_2 at the conical intersection seam mediated by the particular vibronic mode excitation.

Herein, conical intersection seam generated by the bound S_1 ($\pi\pi^*$) and continuum S_2 ($\pi\sigma^*$) states, encountered along an ultrafast S-D bond rupture of thiophenol-d_1, has been experimentally probed. It is manifested by a striking variation of the anisotropy parameter (β) of the fragment angular distribution as a function of the excitation energy, which is attributed to the coherent excitation of the bound S_1 and unbound S_2 in the conical intersection region. The peak in β is ascribed to in-plane S-D bending mode excitation by which the nuclear configuration in the proximity of the S_1/S_2 conical intersection seam is accessed, showing a mixed character of parallel (S_1-S_0) and perpendicular (S_2-S_0) transition dipole moments at the same time. As a result, the conical intersection, which acts as a dynamic funnel for the nonadiabatic reaction, has been spectroscopically characterized through direct access to the nuclear configuration near the conical intersection seam, unraveling the nature of the complicated nonadiabatic surface crossing structures and dynamics of the multidimensional polyatomic system.

■ ASSOCIATED CONTENT

Supporting Information

The Supporting Information is available free of charge on the ACS Publications website at DOI: 10.1021/acs.jpclett.5b01420.

Details of experimental methods; Franck−Condon simulation spectra; anharmonic vibrational frequencies in the ground state; PHOFEX spectrum of thiophenol-h_1; center and side PHOFEX spectra; the simulation of PHOFEX spectrum; the plot of $\tilde{X}/\tilde{A}$ branching ratios, anisotropy parameter (β), and the fraction (Γ, $S_2/(S_1+S_2)$); calculated energies and geometrical parameters of the S_1/S_2 CI seam; calculated gradient difference and derivative coupling motions for the S_1/S_2 CI seam; vertical excitation energies, oscillator strength, and TDM; and molecular orbitals used for the CASSCF calculations. (PDF)

■ AUTHOR INFORMATION

Corresponding Author

*E-mail: sangkyukim@kaist.ac.kr.

Present Address

‡S.H.: Max-Born-Institute for Nonlinear Optics and Short Pulse Spectroscopy in Berlin Research Association, Max-Born-Str. 2A, 12489 Berlin, Germany

Author Contributions

†H.S.Y. and S.H. contributed equally.

Notes

The authors declare no competing financial interest.

■ ACKNOWLEDGMENTS

This work has been supported by the Samsung Science and Technology Foundation under Project Number SSTF-BA1401-09.

■ REFERENCES

(1) Born, M.; Oppenheimer, R. On the Quantum Theory of Molecules. *Ann. Phys.* **1927**, *84*, 457−484.

DOI: 10.1021/acs.jpclett.5b01420
J. Phys. Chem. Lett. 2015, 6, 3202−3208

(2) Worth, G. A.; Cederbaum, L. S. Beyond Born-Oppenheimer: Molecular Dynamics through a Conical Intersection. *Annu. Rev. Phys. Chem.* **2004**, *55*, 127−158.
(3) Yarkony, D. R. Nonadiabatic Quantum Chemistry—Past, Present, and Future. *Chem. Rev.* **2012**, *112*, 481−498.
(4) Tully, J. C. Perspective: Nonadiabatic Dynamics Theory. *J. Chem. Phys.* **2012**, *137*, 22A301.
(5) Polli, D.; Altoè, P.; Weingart, O.; Spillane, K. M.; Manzoni, C.; Brida, D.; Tomasello, G.; Orlandi, G.; Kukura, P.; Mathies, R. A.; Garavelli, M.; Cerullo, G. Conical Intersection Dynamics of the Primary Photoisomerization Event in Vision. *Nature* **2010**, *467*, 440−443.
(6) Zgrablić, G.; Novello, A. M.; Parmigiani, F. Population Branching in the Conical Intersection of the Retinal Chromophore Revealed by Multipulse Ultrafast Optical Spectroscopy. *J. Am. Chem. Soc.* **2011**, *134*, 955−961.
(7) Domcke, W.; Yarkony, D. R.; Köppel, H. *Conical Intersections: Electronic Structure, Dynamics and Spectroscopy*; World Scientific: Singapore, 2004.
(8) Domcke, W.; Yarkony, D. R.; Köppel, H. *Conical Intersections: Theory, Computation and Experiment*; World Scientific: Singapore, 2011.
(9) Domcke, W.; Yarkony, D. R. Role of Conical Intersections in Molecular Spectroscopy and Photoinduced Chemical Dynamics. *Annu. Rev. Phys. Chem.* **2012**, *63*, 325−352.
(10) Serrano-Pérez, J. J.; de Vleeschouwer, F.; de Proft, F.; Mendive-Tapia, D.; Bearpark, M. J.; Robb, M. A. How the Conical Intersection Seam Controls Chemical Selectivity in the Photocycloaddition of Ethylene and Benzene. *J. Org. Chem.* **2012**, *78*, 1874−1886.
(11) Garavelli, M.; Celani, P.; Bernardi, F.; Robb, M. A.; Olivucci, M. The $C_5H_6NH_2^+$ Protonated Shiff Base: An ab Initio Minimal Model for Retinal Photoisomerization. *J. Am. Chem. Soc.* **1997**, *119*, 6891−6901.
(12) Polli, D.; Weingart, O.; Brida, D.; Poli, E.; Maiuri, M.; Spillane, K. M.; Bottoni, A.; Kukura, P.; Mathies, R. A.; Cerullo, G.; Garavelli, M. Wavepacket Splitting and Two-Pathway Deactivation in the Photoexcited Visual Pigment Isorhodopsin. *Angew. Chem., Int. Ed.* **2014**, *53*, 2504−2507.
(13) Sobolewski, A. L.; Domcke, W.; Dedonder-Lardeux, C.; Jouvet, C. Excited-State Hydrogen Detachment and Hydrogen Transfer Driven by Repulsive $^1\pi\sigma^*$ States: A New Paradigm for Nonradiative Decay in Aromatic Biomolecules. *Phys. Chem. Chem. Phys.* **2002**, *4*, 1093−1100.
(14) Asturiol, D.; Lasorne, B.; Worth, G. A.; Robb, M. A.; Blancafort, L. Exploring the Sloped-to-Peaked S_2/S_1 Seam of Intersection of Thymine with Electronic Structure and Direct Quantum Dynamics Calculations. *Phys. Chem. Chem. Phys.* **2010**, *12*, 4949−4958.
(15) Lan, Z.; Domcke, W.; Vallet, V.; Sobolewski, A. L.; Mahapatra, S. Time-Dependent Quantum Wave-Packet Description of the $^1\pi\sigma^*$ Photochemistry of Phenol. *J. Chem. Phys.* **2005**, *122*, 224315.
(16) Venkatesan, T. S.; Ramesh, S. G.; Lan, Z.; Domcke, W. Theoretical Analysis of Photoinduced H-atom Elimination in Thiophenol. *J. Chem. Phys.* **2012**, *136*, 174312−174316.
(17) Böhm, M.; Tatchen, J.; Krügler, D.; Kleinermanns, K.; Nix, M. G. D.; LeGreve, T. A.; Zwier, T. S.; Schmitt, M. High-Resolution and Dispersed Fluorescence Examination of Vibronic Bands of Tryptamine: Spectroscopic Signatures for L_a/L_b Mixing near a Conical Intersection. *J. Phys. Chem. A* **2009**, *113*, 2456−2466.
(18) Lim, J. S.; Lee, Y. S.; Kim, S. K. Control of Intramolecular Orbital Alignment in the Photodissociation of Thiophenol: Conformational Manipulation by Chemical Substitution. *Angew. Chem., Int. Ed.* **2008**, *47*, 1853−1856.
(19) Oliver, T. A. A.; King, G. A.; Tew, D. P.; Dixon, R. N.; Ashfold, M. N. R. Controlling Electronic Product Branching at Conical Intersections in the UV Photolysis of para-Substituted Thiophenols. *J. Phys. Chem. A* **2012**, *116*, 12444−12459.
(20) Han, S.; You, H. S.; Kim, S.-Y.; Kim, S. K. Dynamic Role of the Intramolecular Hydrogen Bonding in Nonadiabatic Chemistry Revealed in the UV Photodissociation Reactions of 2-Fluorothiophenol and 2-Chlorothiophenol. *J. Phys. Chem. A* **2014**, *118*, 6940−6949.
(21) Han, S.; Lim, J. S.; Yoon, J.-H.; Lee, J.; Kim, S.-Y.; Kim, S. K. Conical Intersection Seam and Bound Resonances Embedded in Continuum Observed in the Photodissociation of Thioanisole-d_3. *J. Chem. Phys.* **2014**, *140*, 054307.
(22) Roberts, G. M.; Hadden, D. J.; Bergendahl, L. T.; Wenge, A. M.; Harris, S. J.; Karsili, T. N. V.; Ashfold, M. N. R.; Paterson, M. J.; Stavros, V. G. Exploring Quantum Phenomena and Vibrational Control in σ^* Mediated Photochemistry. *Chem. Sci.* **2013**, *4*, 993−1001.
(23) Grebenshchikov, S. Y.; Qu, Z. W.; Zhu, H.; Schinke, R. New Theoretical Investigations of the Photodissociation of Ozone in the Hartley, Huggins, Chappuis, and Wulf Bands. *Phys. Chem. Chem. Phys.* **2007**, *9*, 2044−2064.
(24) Worner, H. J.; Bertrand, J. B.; Fabre, B.; Higuet, J.; Ruf, H.; Dubrouil, A.; Patchkovskii, S.; Spanner, M.; Mairesse, Y.; Blanchet, V.; Mevel, E.; Constant, E.; Corkum, P. B.; Villeneuve, D. M. Conical Intersection Dynamics in NO_2 Probed by Homodyne High-Harmonic Spectroscopy. *Science* **2011**, *334*, 208−212.
(25) Lim, J. S.; Kim, S. K. Experimental Probing of Conical Intersection Dynamics in the Photodissociation of Thioanisole. *Nat. Chem.* **2010**, *2*, 627−632.
(26) Choi, H.; Park, Y. C.; Lee, Y. S.; An, H.; Baeck, K. K. Theoretical Study of the Extremely Small Torsional Barriers of Thiophenol in the Ground and the First Excited Electronic States. *Chem. Phys. Lett.* **2013**, *580*, 32−36.
(27) Lim, I. S.; Lim, J. S.; Lee, Y. S.; Kim, S. K. Experimental and Theoretical Study of the Photodissociation Reaction of Thiophenol at 243nm: Intramolecular Orbital Alignment of the Phenylthiyl Radical. *J. Chem. Phys.* **2007**, *126*, 034306−034310.
(28) Ashfold, M. N. R.; Devine, A. L.; Dixon, R. N.; King, G. A.; Nix, M. G. D.; Oliver, T. A. A. Exploring Nuclear Motion through Conical Intersections in the UV Photodissociation of Phenols and Thiophenol. *Proc. Natl. Acad. Sci. U. S. A.* **2008**, *105*, 12701−12706.
(29) Devine, A. L.; Nix, M. G. D.; Dixon, R. N.; Ashfold, M. N. R. Near-Ultraviolet Photodissociation of Thiophenol. *J. Phys. Chem. A* **2008**, *112*, 9563−9574.
(30) Lim, J. S.; Choi, H.; Lim, I. S.; Park, S. B.; Lee, Y. S.; Kim, S. K. Photodissociation Dynamics of Thiophenol-d_1: The Nature of Excited Electronic States along the S−D Bond Dissociation Coordinate. *J. Phys. Chem. A* **2009**, *113*, 10410−10416.
(31) Fano, U. Effects of Configuration Interaction on Intensities and Phase Shifts. *Phys. Rev.* **1961**, *124*, 1866−1878.
(32) Tauro, S.; Liu, K. P. Anisotropies of Photoelectron Angular Distribution in the Vicinity of Autoionization Resonances. *J. Phys. B: At., Mol. Opt. Phys.* **2008**, *41*, 225001.
(33) Ahn, D.-S.; Kim, S.-Y.; Lim, G.-I.; Lee, S.; Choi, Y. S.; Kim, S. K. Mode-Dependent Fano Resonances Observed in the Predissociation of Diazirine in the S_1 State. *Angew. Chem., Int. Ed.* **2010**, *49*, 1244−1247.
(34) An, H.; Choi, H.; Lee, Y. S.; Baeck, K. K. Factors Affecting the Branching Ratio of Photodissociation: Thiophenol Studied through Quantum Wavepacket Dynamics. *ChemPhysChem* **2015**, *16*, 1529−1534.

DOI: 10.1021/acs.jpclett.5b01420
J. Phys. Chem. Lett. 2015, 6, 3202−3208